Supplement for

Estuarine Mixing Drives Organic Nitrogen Transformation and Bioavailability Dynamics

Chenglong Han[1], Shaojun Qiu[1], Xinyi Li[1], Ying Ke[1], Rolf D. Vogt[2], Xueqiang Lu[1*]

[1] Tianjin Key Laboratory of Environmental Technology for Complex Trans-media Pollution, Tianjin International Joint Research Center for Environmental Biogeochemical Technology, College of Environmental Science and Engineering, Nankai University, Tianjin 300350, China

[2] Norwegian Institute for Water Research, Oslo 0579, Norway

Contents of this file

Text S1 to S2
Figures S1 to S9
Tables S1 to S4

Text S1. Tangential Flow Ultrafiltration (TFF)

Tangential flow ultrafiltration (TFF) was employed to fractionate dissolved organic nitrogen (DON) in water samples based on molecular weight (MW) ranges. The TFF setup included polyether sulfone (PES) ultrafiltration membrane cartridges (Vivaflow 50, Sartorius, Germany) with nominal molecular weight cutoffs (MWCOs) of 1 kDa and 10 kDa, a MASTERFLEX L/S peristaltic pump, and MASTERFLEX L/S precision polyvinyl chloride (PVC) tubing (Figure S1a). The peristaltic pump maintained tangential flow across the membrane surfaces. A schematic overview of the TFF procedure is shown in Figure S1b.

Prior to TFF, water samples were filtered through a 0.45 μm membrane (Amicrom, 47 mm). The initial TFF step used a 10 kDa membrane to separate the sample into two fractions: DON > 10 kDa (retentate, concentrated to 100–150 mL) and DON < 10 kDa (permeate). The DON < 10 kDa fraction was further processed with a 1 kDa membrane, yielding two additional fractions: DON 1–10 kDa (retentate, 100–150 mL) and DON < 1 kDa (final permeate). All retentates and ultrafiltrates were collected in 50 mL centrifuge tubes for subsequent analysis of DON and dissolved inorganic nitrogen (DIN).

To avoid overestimation of colloidal nitrogen due to potential retention of DON < 1 kDa, the colloidal fraction was calculated using an ultrafiltration permeation model. Based on previous studies and our preliminary experiments, when the concentration factor (CF) was ≥ 30, the difference between model-based and observed colloidal nitrogen abundance remained within 5% (Yang et al., 2021). Therefore, a uniform CF of 30 was applied to all samples to reduce analytical variability and facilitate inter-sample comparisons. The CF was calculated using Equation 1:

$$CF = \frac{Total\ Sample\ Volume}{Retentate\ Volume} \qquad Equation\ 1$$

To minimize cross-contamination, a six-step cleaning protocol was applied to the TFF system before each experiment and between successive samples. The protocol involved sequential rinsing with:

- 1% Micro-90 detergent,
- Milli-Q water,
- mol L^{-1} NaOH,
- Milli-Q water,
- mol L^{-1} HCl, and
- Milli-Q water,

with each step lasting 20 minutes. After cleaning, Milli-Q water was run through the tubing, and its nitrate concentration was measured using an ultraviolet-visible spectrophotometer (TU-1901, Persee, China). The cleaning was deemed complete only when the nitrate concentration was below the detection limit of the nitrogen oxides analyzer.

To ensure quality control, nitrogen recovery efficiency was evaluated and found to range between 80–120% (Figure S1c), consistent with acceptable limits (Powell et al., 1996). The following equations were used for calculations:

$$C_C = C_{pu} - C_u \qquad Equation\ 2$$

$$R = \frac{C_u(CF - 1) + C_{if}}{CF \times C_{pu}} \times 100 \qquad Equation\ 3$$

where, C_{pu}, C_{if}, C_u, and C_c represent the nitrogen concentrations. C_{pu}: Nitrogen concentration in the pre-filtered sample. C_{if}: Nitrogen concentration in the retentate. C_u: Nitrogen concentration in the ultrafiltrate. Cc: Colloidal nitrogen concentration. R: Colloidal nitrogen recovery efficiency

To purify the CON fraction and remove free small molecules and ions, CON-enriched concentrates were dialyzed against 3 L of double-distilled water using 1000 Da MWCO dialysis membranes (HF132640, Henghuibio), under continuous magnetic stirring for 24 h (Ouyang et al., 2018).

Text S2. Sample analysis precision, detection limits, and quality control

The concentrations of dissolved organic carbon (DOC) and total dissolved nitrogen (TDN) were measured using high-temperature catalytic oxidation with a TOC analyzer (multi N/C 3100, Analytik Jena, Germany) equipped with a TDN module. The method had a detection limit of 4 μg L^{-1} and a measurement precision of 2%. Quality control involved periodic analysis of ultrapure water blanks and reference standards (1.0 mg L^{-1} potassium hydrogen phthalate for DOC; 0.5 mg L^{-1} KNO_3 + 0.5 mg L^{-1} urea for TDN) every fifth sample, with recovery efficiencies exceeding 97% (Ye et al., 2018). DON was calculated as the difference between TDN and dissolved inorganic nitrogen (DIN). DIN species were quantified using standard marine nutrient analysis protocols and a UV-Vis spectrophotometer (TU-1901, Persee, China), with detection limits of 0.3 μg L^{-1}, 0.7 μg L^{-1} and 0.4 μg L^{-1} and relative standard deviations (RSDs) of < 4%, < 3%, and < 2% for NO_2^-, NO_3^-, and NH_4^+, respectively (Wu et al., 2023). Using the procedure described above, concentrations of total nitrogen and inorganic nitrogen in the truly dissolved fraction (<1 kDa) were determined concurrently. tDON was similarly calculated as the difference between total nitrogen and inorganic nitrogen in this fraction. CON concentrations were calculated by subtracting tDON from DON, based on a sufficiently high concentration factor (≥ 30) during filtration (Yang et al., 2021) as elaborated in the Supplementary Information. Measurement uncertainties arising from subtraction and addition were estimated using the error propagation method described by Cornell et al. (2003). All samples were analyzed in triplicate, with analytical accuracy consistently exceeding 95 %.

Particulate nitrogen (PN), particulate organic carbon (POC), and stable isotope ratios ($\delta^{13}C$, $\delta^{15}N$) were analyzed in continuous-flow mode using an elemental gas analyzer coupled to an isotope ratio mass spectrometer (DELTA V Advantage, Thermo Fisher Scientific, USA). Prior to analysis, filters containing particulate matter were acidified with ~1 mL of 1 mol L^{-1} HCl to remove carbonates. This treatment had a negligible effect on PN and $\delta^{15}N$ measurements, and has been applied in previous studies (Loick et al., 2007; Kao et al., 2012; Yan et al., 2022). POC and PN on dried filters were quantified after combustion in tin capsules using L-cystine as the calibration standard, with analytical accuracies exceeding 99% and 97.5%, respectively. Isotopic values were calibrated against the Pee Dee Belemnite standard for $\delta^{13}C$ and atmospheric N_2 for $\delta^{15}N$ (Wu et al., 2023), with measurement precisions of ±0.1‰ and ±0.2‰, respectively. Particulate inorganic nitrogen (PIN) was determined using standard nutrient analysis methods after a 2-hour oscillatory extraction with 25 mL of 0.1 M HCl (Zuo et al., 2016). As PIN accounted for less than 5% of total PN, PN was considered equivalent to PON in this study.

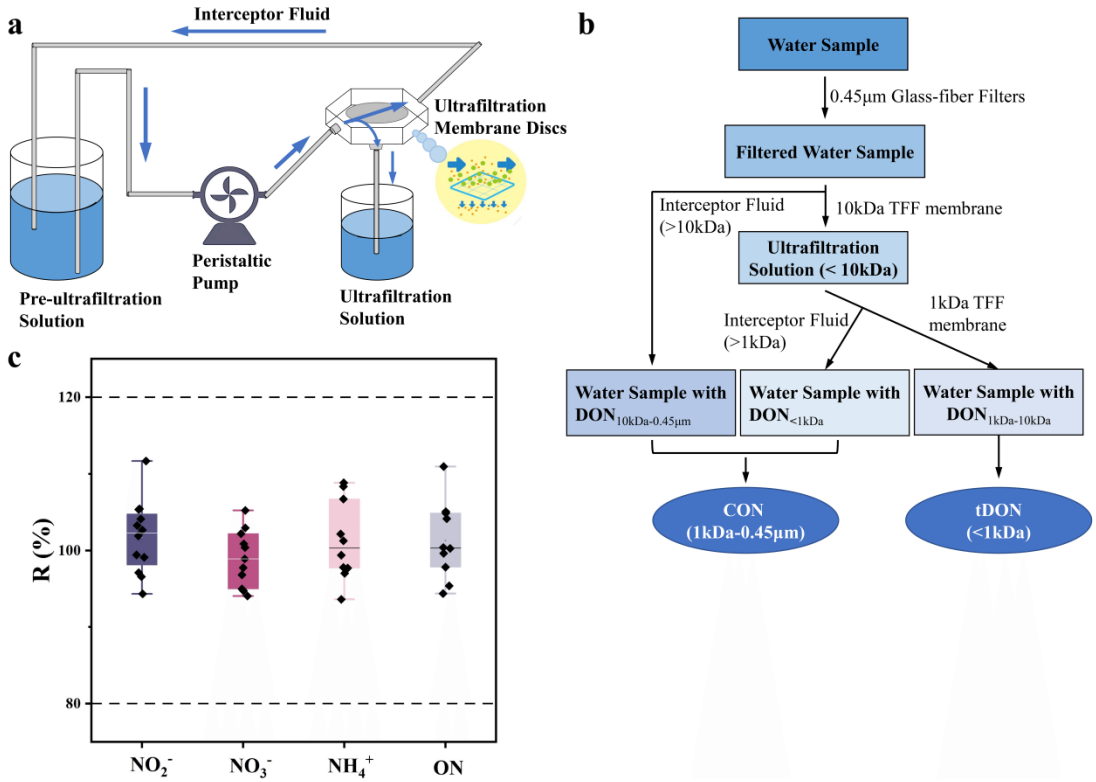

Figure S1. Schematic diagram of Tangential Flow Ultrafiltration (TFF) device (a) and process of TFF (b). Mass recovery of colloidal nitrogen from TFF device (c).

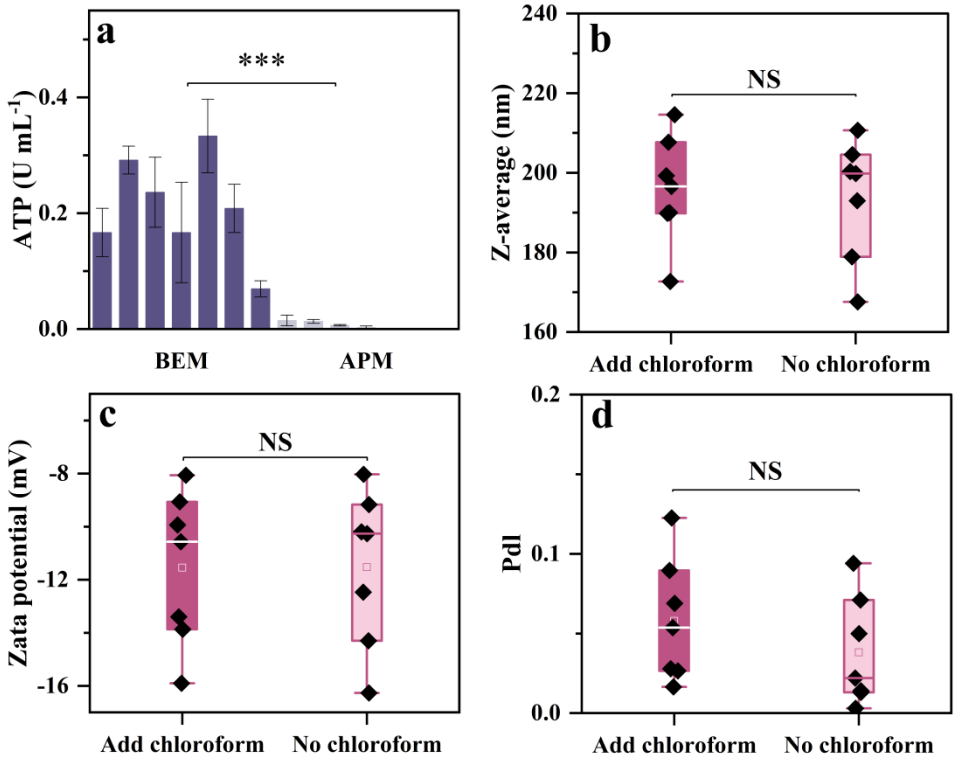

Figure S2. ATPase activity in the biologically active mixing (BAM) and biologically inhibited mixing (i.e., physicochemical mixing only, BIM) treatments (a). ATPase activity was

significantly higher in the BAM treatments ($p < 0.001$), with near-zero activity in the BIM treatments, validating the effectiveness of the inhibition. Potential interference by chloroform was assessed by conducting a 2 h experiment evaluating flocculation and/or adsorption of amino sugar (a representative DON component, 1 mg L^{-1}) in a turbid suspension (50 mg L^{-1} SPM). The effect of addition/non-addition of chloroform on the average particle size (b), Zeta potential (c) and Pdl (d) of the amino sugar (1 mg L^{-1}) + inactivated SPM (50 mg L^{-1}) system was examined, oscillating at 180 *rpm* for 2 hours. NS means no significance, and '***' denotes $p < 0.001$. Zeta potential analysis showed no significant changes in average particle size, zeta potential, or Phl following chloroform addition (Figure S2, $p > 0.05$), indicating minimal interference in the observed ON behavior during the experiments.

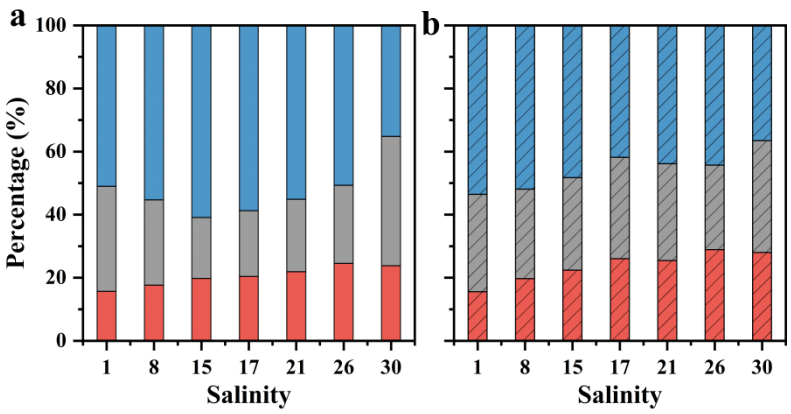

Figure S3. Variations of proportions of different organic nitrogen forms along varying ratios of estuarine mixing in the biologically active mixing (BAM) (a) and biologically inhibited mixing (i.e., physicochemical mixing only, BIM) treatments (b). Red represents particulate organic nitrogen (PON), gray represents colloidal organic nitrogen (CON), and blue represents truly dissolved organic nitrogen (tDON).

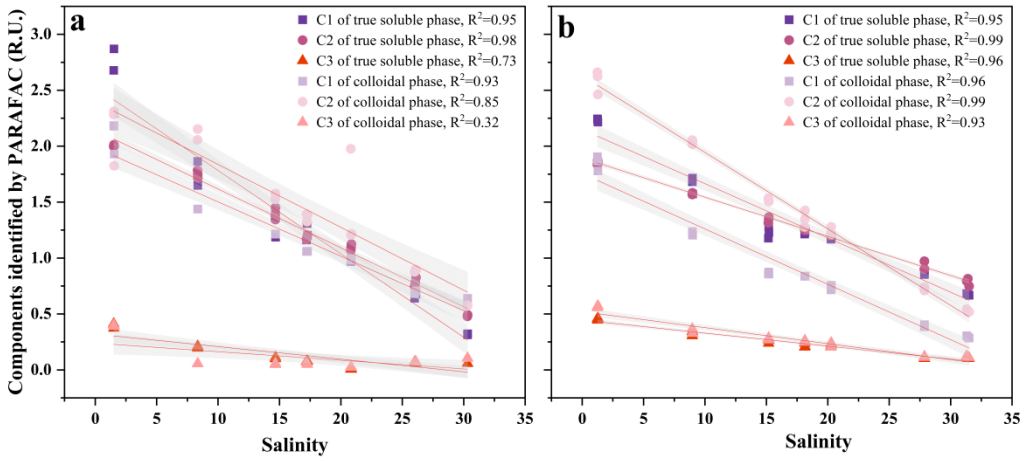

Figure S4. The relationship of salinity and three components identified by PARAFAC in the biologically active mixing (BAM) (a) and biologically inhibited mixing (i.e., physicochemical mixing only, BIM) treatments (b). Shaded areas represent 95% confident intervals.

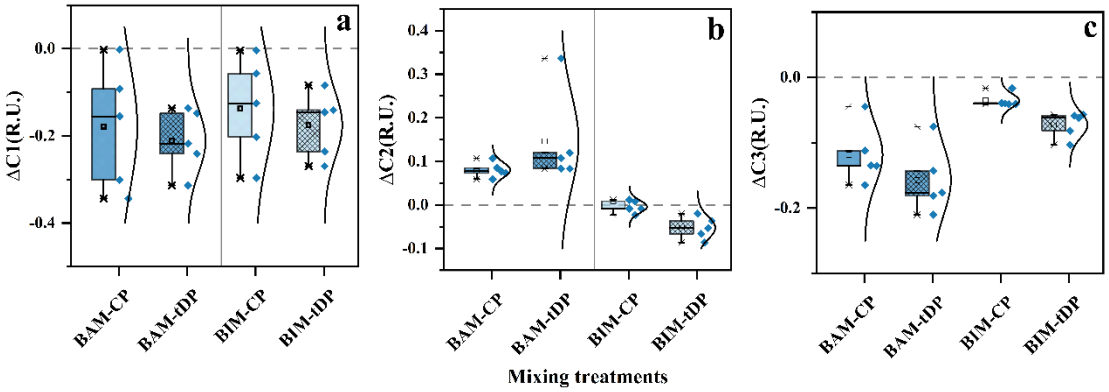

Figure S5. Comparison of relative intensity changes of C1, C2, and C3 at the truly dissolved phase (tDP) and the colloidal phase (CP) of the biologically active mixing (BAM) (a) and biologically inhibited mixing (i.e., physicochemical mixing only, BIM) treatments (b). Blue diamonds represent the samples (n = 5), and squares show the mean values. NS means no significance, and '***' denote $p < 0.001$.

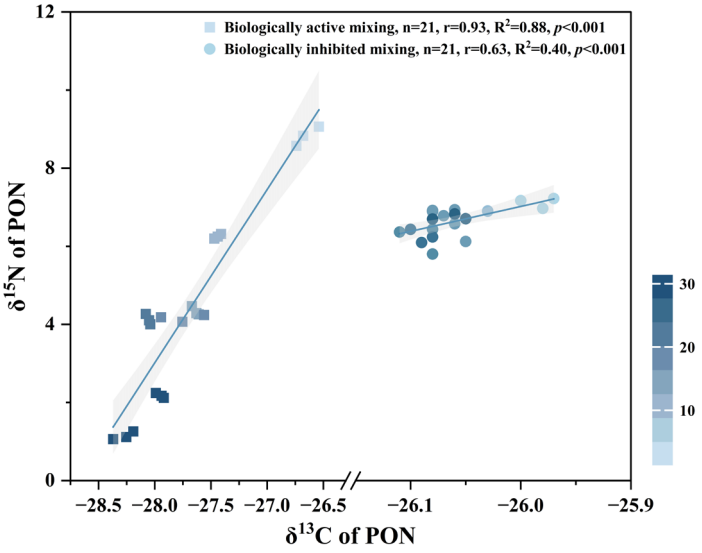

Figure S6. The relationship of $\delta^{13}C$ and $\delta^{15}N$ of PON in two mixing treatments.

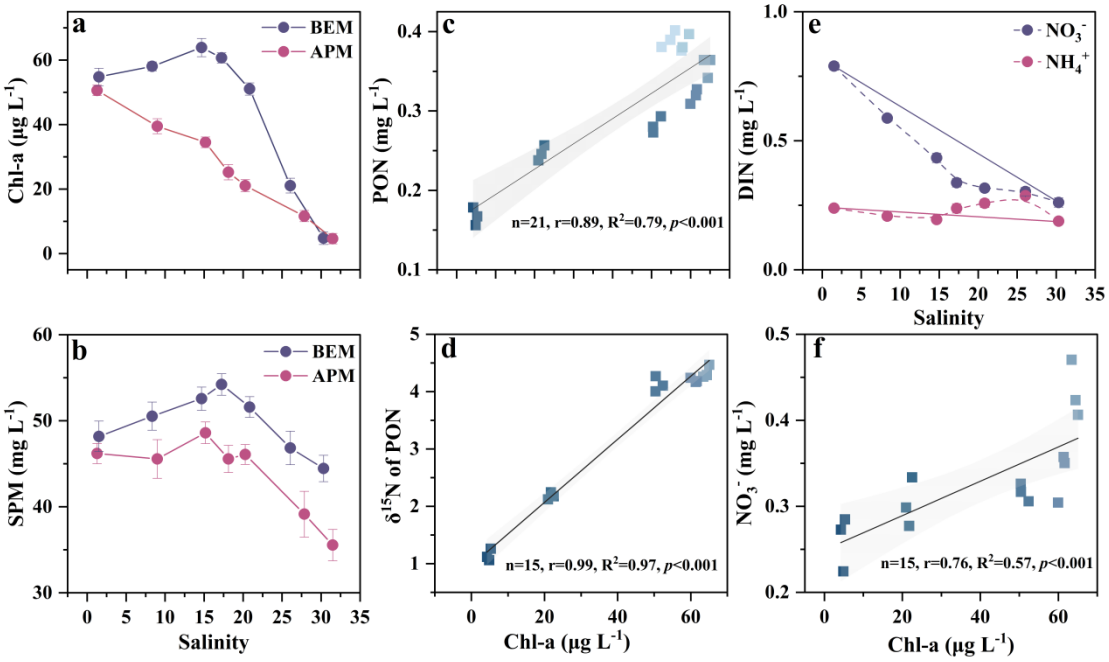

Figure S7. Variations of (a) Chl-a, (b) Suspended Particulate Matter (SPM), (e) nitrate (NO_3^-) and ammonium (NH_4^+) along the salinity gradient in the biologically active mixing (BAM) and biologically inhibited mixing (i.e., physicochemical mixing only, BIM) treatments (a, b). The relationship of (c) Chl-a and PON, (d) Chl-a and $\delta^{15}N$ of PON, (f) Chl-a and NO_3^- in the BAM treatments.

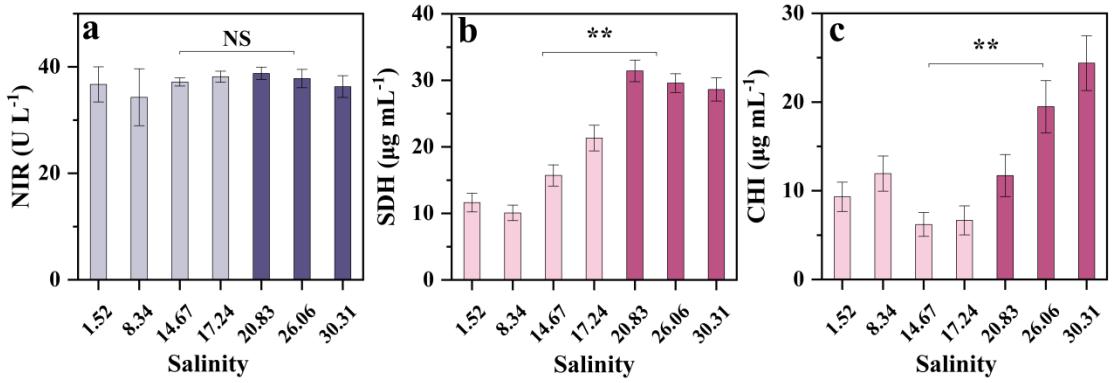

Figure S8. Variations in the activities of (a) nitrite reductase (NIR), (b) succinate dehydrogenase (SDH), and (c) chitinase (CHI) along varying ratios of estuarine mixing in the biologically active mixing treatments. NS means no significance, and '**' doenotes $p < 0.01$.

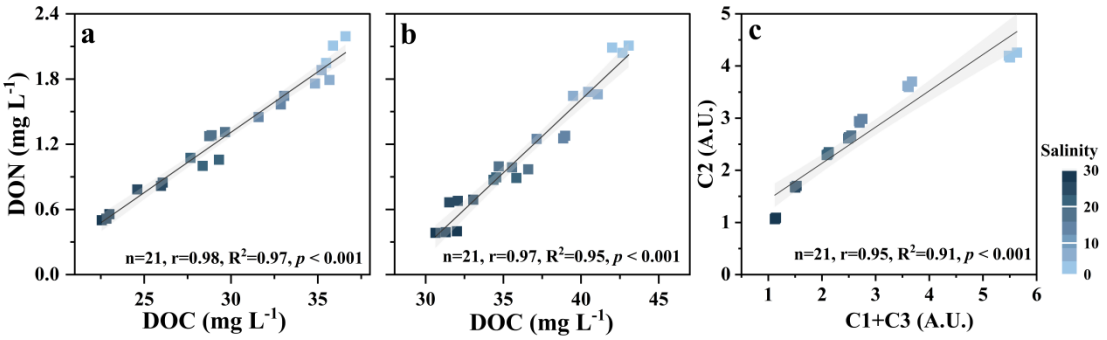

Figure S9. The relationship of DOC and DON in the biologically active mixing (a) and biologically inhibited mixing (i.e., physicochemical mixing only) treatments (b). The relationship of protein-like (C2) and humic-like (C1+C3) in the biologically active mixing treatments (c).

Table S1. Sampling information, physicochemical properties of river water and seawater, and mineral composition of suspended particulate matter (SPM) in New Ziya Riverway and Bohai Bay.

	New Ziya Riverway	**Bohai Bay**
Sampling data	2024.7	2024.7
Sampling coordinates	117.250°E, 38.602°N; 117.257°E, 38.601°N; 117.262°E, 38.603°N	118.160°E, 38.662°N; 118.186°E, 38.670°N 118.171°E, 38.660°N
Temperature (℃)	17.0 ± 2.3	18.5 ± 1.4
Salinity	0.49 ± 0.11	31.52 ± 0.20
pH	7.87 ± 0.03	8.20 ± 0.05
SPM (mg L^{-1})	45.2 ± 4.35	20.1 ± 3.46
DO (mg L^{-1})	9.10 ± 0.47	9.12 ± 0.36
TOC (mg L^{-1})	44.77 ± 3.68	32.16 ± 4.32
TN (mg L^{-1})	3.64 ± 1.34	1.14 ± 0.24
DIN (mg L^{-1})	1.54 ± 1.12	0.60 ± 0.21
DON (mg L^{-1})	2.10 ± 1.45	0.54 ± 0.17
DIP (mg L^{-1})	0.015 ± 0.003	0.011 ± 0.001
Quartz (%)	27	/
Potash feldspar (%)	4	/
Illite (%)	48	/
Chlorite (%)	3	/
Calcite (%)	2	/
Dolomite (%)	8	/
Plagioclase (%)	8	/

Table S2. Variation in the concentrations and compositions of truly dissolved organic carbon (tDON), colloidal organic nitrogen (CON) and particulate organic nitrogen (PON).

Salinity	PON (mg L^{-1})	CON (mg L^{-1})	tDON (mg L^{-1})	CON compounds-RI			tDON compounds-RI			Relative theoretical dilution curve offset percentage (%)		δ^{15}N-PON (‰)	δ^{13}C-PON (‰)
				C1	C2	C3	C1	C2	C3	C1+C3	C2		
Biologically active mixing (i.e., biological and physicochemical processes occurring concurrently, BAM)													
1.52	0.391	0.829	1.270	2.61	2.00	0.40	2.10	2.14	0.40	/	/	8.82	-26.65
8.34	0.387	0.622	1.210	1.77	1.70	0.21	1.44	2.11	0.18	19.46	11.58	6.29	-27.44
14.67	0.358	0.439	1.101	1.22	1.40	0.11	1.21	1.53	0.05	25.88	7.04	4.34	-27.64
17.24	0.317	0.386	0.913	1.21	1.25	0.08	1.06	1.37	0.06	22.89	6.53	4.20	-27.75
20.83	0.282	0.359	0.709	0.98	1.09	0.01	0.98	1.21	0.03	22.21	10.9	4.13	-27.86
26.06	0.244	0.297	0.504	0.66	0.78	0.06	0.71	0.89	0.07	15.27	10.27	1.38	-27.95
30.31	0.167	0.289	0.247	0.32	0.49	0.06	0.64	0.57	0.11	/	/	1.15	-28.28
Biologically inhibited mixing (i.e., physicochemical processes mixing only, BIM)													
1.28	0.381	0.756	1.309	2.21	1.86	0.45	1.85	2.58	0.56	/	/	7.12	-25.98
8.98	0.351	0.504	0.924	1.62	1.58	0.32	1.22	2.04	0.35	14.22	0.81	6.87	-26.04
15.18	0.293	0.382	0.630	1.21	1.35	0.25	0.87	1.57	0.28	20.89	2.99	6.88	-26.07
18.13	0.276	0.340	0.443	1.23	1.26	0.22	0.82	1.38	0.26	13.26	2.48	6.53	-26.06
20.27	0.243	0.293	0.418	1.19	1.20	0.22	0.73	1.24	0.22	10.47	1.66	6.20	-26.09
27.85	0.195	0.180	0.298	0.86	0.93	0.11	0.40	0.74	0.11	11.15	1.66	6.25	-26.09
31.5	0.153	0.193	0.199	0.68	0.80	0.11	0.29	0.53	0.12	/	/	6.74	-26.06

Table S3. Compositions and fluorescence characteristics of DOM in the mixed water of New Ziya Riverway and Bohai Bay.

Compositions	Ex/Em (nm)	Characteristics	References
C1	385/478	Terrestrial humic-like component, high molecular weight, aromatic, fluoresces like fulvic acid, widespread	(Osburn et al., 2011; Wang et al., 2022)
C2	305/350	Autochthonous tyrosine, protein-like substances, related to the degradability of DOM	(Liu et al., 2024; Maurischat et al., 2022; Ren et al., 2021)
C3	240/426	microbial humic-like, low molecular weight, related to biological activity	(Fellman et al., 2010; Liu et al., 2025)

Table S4. Global concentrations of salinity, chlorophyll-a and different fractions of nitrogen in different estuaries. Dissolved organic nitrogen (DON) (< 0.45 μm) was divided into truly dissolved organic nitrogen (< 1 kDa) and colloidal organic nitrogen (1 kDa - 0.45 μm). Empty values were not reported.

Serial No.	Estuary	Salinity	Chl-a (μg L^{-1})	DIN (μM)	DON (μM)	tDON (μM)	CON (μM)	PON (μM)	TN (μM)	References
1	Yangtze River Estuary (YRE)	2.2-33.8	0.9-72.4 (9.6)	0.2-150.3 (26.5)	4.4-32.7 (9.8)			0.2-140.8 (9.6)	12.8-301 (49.6)	(Yan et al., 2022)
2	Pearl River Estuary (PRE)		0.92-5.6 (3.3)		29.2-24.7 (26.9)					(Li et al., 2024)
3	Pearl River Estuary (PRE)	5.1-33.7	1.1-2.4 (1.6)	5.6-178.8 (77.0)	11.9-65.5 (27.3)					(Li et al., 2023)
4	Ochlockonee Estuary (OE)	0.03-28.5			8.5-69.9 (29.8)	3.6-31 (14.1)	3.1-57.1 (15.7)			(Powell et al., 1996)
5	West Neck Bay (WNB)		3.3-26.3 (13.2)	0.13-24.9 (3.7)	1.3-10.1 (4.7)	0.5-7.0 (2.8)	0.67-3.9 (2.0)	0.87-15.2 (6.9)	5.3-27.4 (15.7)	(Gobler and Sañudo-Wilhelmy, 2003)
6	Delaware Estuary (DE)	0.11-29.5	1.7-21.6 (10.1)				32.1-48.6 (39.1)	7.4-30.6 (17.0)		(Mannino and Harvey, 2000)
7	York River Estuary (YORE)	4.1-15.8	4.0-60.0 (20.7)	2.0-41,7 (13.5)	8.0-22.5 (15.7)					(Detweiler et al., 2025)
8	Yellow River (YR)			181.9-575.8 (279.1)	11.0-29.6 (17.5)	10.3-30.4 (16.4)	0.37-2.0 (1.2)			(Yan et al., 2021)
9	the North Australian shelf	28.0-36.0			3.9-7.2 (5.9)	3.6-4.2 (3.9)	0.1-3.6 (1.9)			(Knapp et al., 2012)
10	Indian Monsoonal Estuaries (IMEs)	0.04-28.8	0.91-6.8 (3.1)	4.3-24.0 (9.4)				5.9-60.4 (25.1)		(Sarma et al., 2014)
11	Mississippi River Estuary (MRE)				13.0-19.3 (16.2)	6.6-10.5 (8.9)	4.8-11.8 (7.3)			(Duan et al., 2007)
12	Pearl River Estuary (PRE)	0.1-33.3	0.86-35.0 (7.2)	5.2-424.9 (98.3)	7.2-92.7 (40.7)					(Ye et al., 2018)
13	Liaohe River Estuay (LRE)	0.69-30.5	1.1-96.0 (20.0)	48.0-685.6 (278.1)	10.1-240.3 (95.5)			17.6-166.2 (66.7)	107.7-990.7 (440.4)	(Zhang et al., 2014)
14	Brisbane River Estuary (BRE)	1.0-35.8	0.56-18.5 (2.9)	19.4-53.3 (41.0)	28.3-135.6 (52.1)			14.4-48.3 (29.7)	102.7-161.3 (137.1)	(Wells and Eyre, 2019)
15	Maroochy River Estuary (MRE)	0.71-36.6	1.2-14.1 (6.1)	1.8-19.8 (11.2)	13.8-76.2 (33.6)			1.2-75.6 (31.7)	27.0-164.4 (70.5)	(Wells and Eyre, 2019)
16	Noosa River Estuary (NRE)	7.1-36.7	0.28-6.0 (1.6)	5.3-57.7 (12.3)	9.6-32.3 (21.1)			1.3-67.8 (25.7)	20.9-114.4 (59.1)	(Wells and Eyre, 2019)
17	Cape Fear River Estuary	0.2-34.8	0.9-22.3	0.64-101.4	11.6-139.2	10.8-48.6	0.9-101.4			(Dafner et al., 2007)

	(CFRE)		(6.7)	(15.6)	(44.7)	(29.1)	(15.6)			
18	Tampa Bay Estuary (TBE)	0.47-34.2		3.1-14.4 (7.6)	17.2-50.4 (36.7)			8.7-19.1 (12.4)	34.3-79.2 (56.7)	(Jani and Toor, 2018)
19	Wailoa and Wailuku River estuaries (WWRE)	18.9-34.5	0.13-5.56 (1.4)	0.7-14.8 (4.5)	5.0-11.1 (7.4)			1.3-5.5 (2.7)	8.6-22.9 (14.6)	(Wiegner et al., 2013)
20	Manko Estuary (ME)	0.85-29.0	1.1-10.3 (3.7)	49.2-316.4 (168.1)				0.09-2.17 (0.56)		(Shilla et al., 2011)
21	Cachoeira River Estuary (CRE)	1.2-22.8			75.0-275.1 (169.0)					(dos Santos et al., 2018)
22	Elbe River Estuary (ERE)	0.34-30.8	4.3-24.1(8.1)	88.7-153.9 (133.2)	21.2-60.2 (36.6)			17.5-93.4 (42.1)	157.9-200.3 (175.8)	(Dähnke et al., 2022)
23	Hooghly Estuary (HE)	3.5-25.6			3.6-8.3 (5.2)			1.5-5.6 (3.3)		(Fischer et al., 2016)
24	Danshuei River Estuary (DRE)	0.08-32.2	0.93-44.1 (9.2)	11.7-578.1 (229.7)	3.0-110.6 (33.9)			0.50-65.6 (8.4)	18.8-745.0 (275.8)	(Fang and Chen, 2021)

References

Cornell, S. E., Jickells, T. D., Cape, J. N., Rowland, A. P., and Duce, R. A.: Organic nitrogen deposition on land and coastal environments: a review of methods and data, Atmos. Environ., 37, 2173–2191, https://doi.org/10.1016/S1352-2310(03)00133-X, 2003.

Dafner, E. V., Mallin, M. A., Souza, J. J., Wells, H. A., and Parsons, D. C.: Nitrogen and phosphorus species in the coastal and shelf waters of Southeastern North Carolina, Mid-Atlantic U.S. coast, Marine Chem., 103, 289–303, https://doi.org/10.1016/j.marchem.2006.01.008, 2007.

Dähnke, K., Sanders, T., Voynova, Y., and Wankel, S. D.: Nitrogen isotopes reveal a particulate-matter-driven biogeochemical reactor in a temperate estuary, Biogeosciences, 19, 5879–5891, https://doi.org/10.5194/bg-19-5879-2022, 2022.

Detweiler, D. J., Anderson, I. C., Brush, M. J., and Canuel, E. A.: Biogeochemical and physical controls on the microbial degradation of dissolved organic matter along a temperate microtidal estuary, Estuaries Coasts, 48, 51, https://doi.org/10.1007/s12237-024-01474-0, 2025.

Duan, S., Bianchi, T. S., Shiller, A. M., Dria, K., Hatcher, P. G., and Carman, K. R.: Variability in the bulk composition and abundance of dissolved organic matter in the lower Mississippi and Pearl rivers, J. Geophys. Res.-Biogeo., 112, G02024, https://doi.org/10.1029/2006JG000206, 2007.

Fang, T. H. and Chen, W. H.: Dissolved and particulate nitrogen species partitioning and distribution in the Danshuei River estuary, northern Taiwan, Mar. Pollut. Bull., 164, 111981, https://doi.org/10.1016/j.marpolbul.2021.111981, 2021.

Fellman, J. B., Hood, E., and Spencer, R. G. M.: Fluorescence spectroscopy opens new windows into dissolved organic matter dynamics in freshwater ecosystems: A review, Limnol. Oceanogr., 55, 2452–2462, https://doi.org/10.4319/lo.2010.55.6.2452, 2010.

Fischer, P., Unger, D., Palit, A., Einsporn, M. H., and Lara, R. J.: Dissolved inorganic nutrients, organic matter and stable nitrogen isotopes as indicators of human impact in two contrasting estuaries in West Bengal, India, during winter monsoon, Indian J. Geo-Mar. Sci., 45, 16–28, 2016.

Gobler, C. J. and Sañudo-Wilhelmy, S. A.: Cycling of colloidal organic carbon and nitrogen during an estuarine phytoplankton bloom, Limnol. Oceanogr., 48, 2314–2320, https://doi.org/10.4319/lo.2003.48.6.2314, 2003.

Jani, J. and Toor, G. S.: Composition, sources, and bioavailability of nitrogen in a longitudinal gradient from freshwater to estuarine waters, Water Res., 137, 344–354, https://doi.org/10.1016/j.watres.2018.02.042, 2018.

Kao, S., Terence Yang, J., Liu, K., Dai, M., Chou, W., Lin, H., and Ren, H.: Isotope constraints on particulate nitrogen source and dynamics in the upper water column of the oligotrophic South China Sea, Global Biogeochem. Cycles, 26, GB004091, https://doi.org/10.1029/2011GB004091, 2012.

Knapp, A. N., Sigman, D. M., Kustka, A. B., Sañudo-Wilhelmy, S. A., and Capone, D. G.: The distinct nitrogen isotopic compositions of low and high molecular weight marine DON, Marine Chem., 136–137, 24–33, https://doi.org/10.1016/j.marchem.2012.05.001, 2012.

Li, J., Wu, Y., Jiang, Z., Liu, S., Ren, Y., Yang, J., Song, X., Huang, X., and He, D.: Terrestrial and biological activities shaped the fate of dissolved organic nitrogen in a subtropical river-dominated estuary and adjacent coastal area, J. Geophys. Res.-Oceans, 128, e2023JC019911, https://doi.org/10.1029/2023JC019911, 2023.

Li, J., Wu, Y., Yang, J., Li, P., Jiang, Z., Liu, S., and Huang, X.: Estuarine hydrodynamic processes driving the molecular changes of terrestrial dissolved organic nitrogen: From mixing to biological modification, Sci. Total Environ., 917, 170489, https://doi.org/10.1016/j.scitotenv.2024.170489, 2024.

Liu, H., Cai, F., Huang, Z., Wang, C., Li, X., Wang, X., and Shen, J.: Seasonal hydrological variation impacts nitrogen speciation and enhances bioavailability in plateau lake sediments, Water Res., 271, 122990, https://doi.org/10.1016/j.watres.2024.122990, 2025.

Liu, X., Lan, C., Zhu, L., Yan, C., Wang, N., Chen, H., Zheng, G., Che, Y., Yang, Z., and Bao, R.: Sediment resuspension as a driving force for organic carbon transference and rebalance in marginal seas, Water Res., 257, 121672, https://doi.org/10.1016/j.watres.2024.121672, 2024.

Loick, N., Dippner, J., Doan, H. N., Liskow, I., and Voss, M.: Pelagic nitrogen dynamics in the Vietnamese upwelling area according to stable nitrogen and carbon isotope data, DEEP-SEA RES PT I, 54, 596–607, https://doi.org/10.1016/j.dsr.2006.12.009, 2007.

Mannino, A. and Harvey, H. R.: Biochemical composition of particles and dissolved organic matter along an estuarine gradient: Sources and implications for DOM reactivity, Limnol. Oceanogr., 45, 775–788, https://doi.org/10.4319/lo.2000.45.4.0775, 2000.

Maurischat, P., Lehnert, L., Zerres, V. H. D., Tran, T. V., Kalbitz, K., Rinnan, Å., Li, X. G., Dorji, T., and Guggenberger, G.: The glacial–terrestrial–fluvial pathway: A multiparametrical analysis of spatiotemporal dissolved organic matter variation in three catchments of Lake Nam Co, Tibetan Plateau, Sci. Total Environ., 838, 156542, https://doi.org/10.1016/j.scitotenv.2022.156542, 2022.

Osburn, C. L., Wigdahl, C. R., Fritz, S. C., and Saros, J. E.: Dissolved organic matter composition and photoreactivity in prairie lakes of the U.S. Great Plains, Limnol. Oceanogr., 56, 2371–2390, https://doi.org/10.4319/lo.2011.56.6.2371, 2011.

Ouyang, S., Hu, X., Zhou, Q., Li, X., Miao, X., and Zhou, R.: Nanocolloids in natural water: Isolation, characterization, and toxicity, Environ. Sci. Technol., 52, 4850–4860, https://doi.org/10.1021/acs.est.7b05364, 2018.

Powell, R. T., Landing, W. M., and Bauer, J. E.: Colloidal trace metals, organic carbon and nitrogen in a southeastern U.S. estuary, Marine Chem., 55, 165–176, https://doi.org/10.1016/S0304-4203(96)00054-0, 1996.

Ren, W., Wu, X., Ge, X., Lin, G., Zhou, M., Long, Z., Yu, X., and Tian, W.: Characteristics of dissolved organic matter in lakes with different eutrophic levels in southeastern Hubei Province, China, J. Ocean. Limnol., 39, 1256–1276, https://doi.org/10.1007/s00343-020-0102-x, 2021.

dos Santos, C. B., Silva, M. A. M., de Souza, M. F. L., and da Silva, D. M. L.: Nitrogen distribution in a tropical urbanized estuarine system in northeastern Brazil, Environ. Monit. Assess., 190, 68, https://doi.org/10.1007/s10661-017-6420-6, 2018.

Sarma, V. V. S. S., Krishna, M. S., Prasad, V. R., Kumar, B. S. K., Naidu, S. A., Rao, G. D., Viswanadham, R., Sridevi, T., Kumar, P. P., and Reddy, N. P. C.: Distribution and sources of particulate organic matter in the Indian monsoonal estuaries during monsoon, J. Geophys. Res.-Biogeo., 119, 2095–2111, https://doi.org/10.1002/2014JG002721, 2014.

Shilla, D. J., Tsuchiya, M., and Shilla, D. A.: Terrigenous nutrient and organic matter in a subtropical river estuary, Okinawa, Japan: origin, distribution and pattern across the estuarine salinity gradient, Chem. Ecol., 27, 523–542, https://doi.org/10.1080/02757540.2011.600831, 2011.

Wang, S., Wasswa, J., Feldman, A. C., Kabenge, I., Kiggundu, N., and Zeng, T.: Suspect screening to support source identification and risk assessment of organic micropollutants in the aquatic environment of a Sub-Saharan African urban center, Water Res., 220, 118706, https://doi.org/10.1016/j.watres.2022.118706, 2022.

Wells, N. S. and Eyre, B. D.: $\delta^{15}N$ patterns in three subtropical estuaries show switch from nitrogen "reactors" to "pipes" with increasing degradation, Limnol. Oceanogr., 64, 860–876, https://doi.org/10.1002/lno.11080, 2019.

Wiegner, T. N., Mead, L. H., and Molloy, S. L.: A comparison of water quality between low- and high-flow river conditions in a tropical estuary, Hilo Bay, Hawaii, Estuaries Coasts, 36, 319–333, https://doi.org/10.1007/s12237-012-9576-x, 2013.

Wu, Y., Li, J., Zhang, X., Jiang, Z., Liu, S., Yang, J., and Huang, X.: The distinct phases of fresh-seawater mixing intricately regulate the nitrogen transformation processes in a high run-off estuary: Insight from multi-isotopes and microbial function analysis, Water Res., 247, 120809, https://doi.org/10.1016/j.watres.2023.120809, 2023.

Yan, X., Yang, J., Xu, M., Wang, H., Dai, M., and Kao, S.: Nitrogen isotope constraint on the zonation of multiple transformations between dissolved and particulate organic nitrogen in the Changjiang plume, Sci. Total Environ., 818, 151678, https://doi.org/10.1016/j.scitotenv.2021.151678, 2022.

Yan, Z., Yang, N., Liang, Z., Yan, M., Zhong, X., Zhang, Y., Xu, W., and Xin, Y.: Active dissolved organic nitrogen cycling hidden in large river and environmental implications, Sci. Total Environ., 795, 148882, https://doi.org/10.1016/j.scitotenv.2021.148882, 2021.

Yang, B., Lin, H., Bartlett, S. L., Houghton, E. M., Robertson, D. M., and Guo, L.: Partitioning and transformation of organic and inorganic phosphorus among dissolved, colloidal and particulate phases in a hypereutrophic freshwater estuary, Water Res., 196, 117025, https://doi.org/10.1016/j.watres.2021.117025, 2021.

Ye, F., Guo, W., Wei, G., and Jia, G.: The sources and transformations of dissolved organic matter in the Pearl River Estuary, China, as revealed by stable isotopes, J. Geophys. Res.-Oceans, 123, 6893–6908, https://doi.org/10.1029/2018JC014004, 2018.

Zhang, J., Yu, L., Yao, Q., and Tian, L.: Mixing behavior of nutrients in different seasons at Liaohe Estuary, Environ. Sci., 35, 569–576, https://doi.org/10.13227/j.hjkx.2014.02.033, 2014.

Zuo, J., Song, J., Yuan, H., Li, X., Li, N., and Duan, L.: Particulate nitrogen and phosphorus in the East China Sea and its adjacent Kuroshio waters and evaluation of budgets for the East China Sea Shelf, Cont. Shelf Res., 131, 1–11, https://doi.org/10.1016/j.csr.2016.11.003, 2016.